Pain Networks From the Inside: Spatiotemporal Analysis of Brain Responses Leading From Nociception to Conscious Perception

Hélène Bastuji,[1,2]* Maud Frot,[1] Caroline Perchet,[1] Michel Magnin,[1] and Luis Garcia-Larrea[1,3]

[1]*Central Integration of Pain (NeuroPain) Lab - Lyon Neuroscience Research Center, INSERM U1028; CNRS, UMR5292, Université Claude Bernard, Bron, F-69677, France*
[2]*Unité D'Hypnologie, Service De Neurologie Fonctionnelle Et D'Épileptologie, Hôpital Neurologique, Hospices Civils De Lyon, Bron, F-69677, France*
[3]*Centre D'évaluation Et De Traitement De La Douleur, Hôpital Neurologique, Lyon, France*

Abstract: Conscious perception of painful stimuli needs the contribution of an extensive cortico-subcortical network, and is completed in less than one second. While initial activities in operculo-insular and mid-cingulate cortices have been extensively assessed, the activation timing of most areas supporting conscious pain has barely been studied. Here we used intracranial EEG to investigate the dynamics of 16 brain regions (insular, parietal, prefrontal, cingulate, hippocampal and limbic) during the first second following nociceptive-specific laser pulses. Three waves of activation could be defined according to their temporal relation with conscious perception, ascertained by voluntary motor responses. Pre-conscious activities were recorded in the posterior insula, operculum, mid-cingulate and amygdala. Antero-insular, prefrontal and posterior parietal activities started later and developed during time-frames consistent with conscious voluntary reactions. Responses from hippocampus, perigenual and perisplenial cingulate developed latest and persisted well after conscious perception occurred. Nociceptive inputs reach simultaneously sensory and limbic networks, probably through parallel spino-thalamic and spino-parabrachial pathways, and the initial limbic activation precedes conscious perception of pain. Access of sensory information to consciousness develops concomitant to fronto-parietal activity, while late-occurring responses in the hippocampal region, perigenual and posterior cingulate cortices likely underlie processes linked to memory encoding, self-awareness and pain modulation. *Hum Brain Mapp 37:4301–4315, 2016*. © 2016 Wiley Periodicals, Inc.

Key words: nociceptive stimulus; consciousness; intracerebral EEG; human; pain matrix

Contract grant sponsor: French Society for Pain Evaluation and Therapy; Contract grant number: Translational Research Grant 2012-14; Contract grant sponsor: LABEX CORTEX; Contract grant number: ANR-11-LABX-0042, ANR-11-IDEX-0007; Contract grant sponsor: Region Rhone-Alpes/France; Contract grant number: ARC2 2012-2015; Contract grant sponsor: INSERM Interface.

*Correspondence to: Hélène Bastuji; Central Integration of Pain (NeuroPain) Lab - Lyon Neuroscience Research Center, INSERM U1028; CNRS, UMR5292; Université Claude Bernard, Bron, F-69677, France. E-mail: bastuji@univ-lyon1.fr

Received for publication 20 April 2016; Revised 19 June 2016; Accepted 27 June 2016.

DOI: 10.1002/hbm.23310
Published online 8 July 2016 in Wiley Online Library (wileyonlinelibrary.com).

© 2016 Wiley Periodicals, Inc.

INTRODUCTION

The human pain experience results from the interaction of nociceptive processing with cognitive-emotional modulation and reappraisal [Melzack and Casey, 1968]. Functional imaging studies have consistently dismissed the notion of a single "pain center" in the brain, and instead delineated a set of brain structures—the "pain matrix"—responding systematically to stimuli eliciting pain, and supposedly underlying the subjective pain experience [reviews Apkarian et al., 2005; Garcia-Larrea and Peyron, 2013; Peyron et al., 2000; Tracey and Mantyh, 2007].

Despite much impetus in determining the regions involved in pain processing, precise characterization in time and space of the cerebral events leading from initial cortical reception to the conscious experience of pain remains lacking. The conscious perception of a sensory stimulus cannot be completed in sensory areas, but requires the activation of a widespread cortical network including cortico-cortical interaction of frontal, temporal and parietal cortices [Aru et al., 2012; Del Cul et al., 2007], and probably trans-thalamic routing of cortico-cortical inputs via the associative thalamus [Cappe et al., 2009; Shipp, 2003]. Functional connectivity within a frontoparietal network, in continuous interplay with stimulus-specific sensory areas, is considered an essential signature of the access of sensory information to consciousness [Dehaene et al., 2006; Del Cul et al., 2007; Gross et al., 2004; Haynes et al., 2005; Långsjö et al., 2012]. While reaction times suggest that the cortical processing leading to the perception of a phasic noxious stimulus is completed in less than 1 s [Dusch et al., 2016; Legrain et al., 2009; Perchet et al., 2012; Siedenberg and Treede, 1996], the hemodynamic responses on which the "pain matrix" concept is based[1] integrate neural-related activity during $10-20$ s, and are unlikely to reflect the rapid building up of immediate perceptions [Buckner, 1998; Peyron et al., 2000]. Moreover, these activities cannot discriminate regions involved in the perceptual process from those reflecting post-perceptual activities such as response selection, memory-encoding or integration of external input with self-awareness. Electrophysiology (EEG/MEG) is able to tag the dynamics of neural responses, but non-invasive scalp recordings often lack the necessary spatial resolution to disentangle closely located regions, in particular when multiple areas are simultaneously active [Nunez and Srinivasan, 2006]. Intracortical EEG recordings, on the other hand, allow detecting the precise time activation of the structures where electrodes are implanted [Bastuji et al., 2015; Frot et al., 2008, 2013; Lenz et al., 1998a,b; Ohara et al., 2008], but in most cases only a small number of contacts are exploited, thus giving only a very partial image of the actual spatio-temporal processing.

Here we analyze responses to nociceptive stimuli obtained during the last decade from over 300 intracortical electrode contacts exploring 16 sensory, associative, paralimbic and limbic cortical areas. This unique set of data allowed constructing a spatio-temporal picture of the network activity during the first second following a nociceptive stimulus. The analysis of response timing together with functional inter-areal relationships via phase-coherence generates a comprehensive image of the activities sustaining and giving rise to the initial perception of pain.

METHODS

Patients

Twenty-seven patients with refractory partial epilepsy were included in this study (18 men, 9 women; mean age 30 years, range $19-51$ years). To delineate the extent of the cortical epileptogenic area and to plan a tailored surgical treatment, depth EEG recording electrodes (diameter 0.8 mm; $5-15$ recording contacts 2 mm long, inter-contact interval 1.5 mm) were implanted according to the stereotactic technique of Talairach and Bancaud [1973]. The decision to explore specific areas resulted from the observation via video-EEG of ictal manifestations suggesting the possibility of seizures propagating to, or originating from these regions [Guenot et al., 2001]. This procedure aims at recording spontaneous seizures but also includes the functional mapping of potentially eloquent cortical areas using evoked potentials recordings and cortical electrical stimulation [Ostrowsky et al., 2002; Mazzola et al., 2006]. In agreement with French regulations relative to invasive investigations with direct individual benefit, patients were fully informed about electrode implantation, stereotactic EEG (SEEG), evoked potential recordings, and cortical stimulation procedures used to localize the epileptogenic cortical areas and gave their consent. The laser stimulation paradigm was submitted to, and approved by, the local Ethics Committee (CCPPRB Léon Bérard-Lyon).

Spinothalamic-specific laser stimulation was performed after a minimal delay of 5 days post electrode implantation; at that time antiepileptic drugs had been tapered down (see Table I) with daily dosages at, or slightly under, the minimum of their usual therapeutic range. None of these patients reported pain symptoms before or after the recording session.

Electrode Implantation

Intracerebral electrodes were implanted using the Talairach's stereotactic frame. A cerebral angiography was performed in stereotactic conditions using an X-ray source located 4.85 m away from the patient's head. This

[1]Either BOLD = *Blood Oxygen Level Dependent signal*, reflecting activity-related changes in the ratio between oxygenated and deoxygenated haemoglobin, or ASL = *Arterial Spin Labelling signal*, quantifying regional blood flow.

TABLE I. Individual clinical, MRI, and SEEG data

Patient	Gender/Age	Treatment	MRI	Seizure onset	Number of Electrodes
P1	M/19	Carbamazepin 800 Valproate 500 Clobazam 10	R fronto-orbital	R fronto-orbital	11/R
P2	F/23	Levetiracetam 2000 Lamotrigin 800	L hippocampal atrophy	L mesial temporal	11/L
P3	F/37	Carbamazepin 600 Pregabalin 75	Normal	L mesial temporal	13/L
P4	M/26	Carbamazepin 200 Lamotrigin 200 Pregabalin 75	L hippocampal atrophy	L mesial temporal	12/L
P5	M/20	None	R hippocampal atrophy	R mesial temporal	12/R
P6	M/21	Topiramate 200 Oxcarbazepin 900 Lamotrigin 400	R temporal dysplasia	R temporal	11/R+3/L
P7	M/39	Lamotrigin 200 Topiramate 200 Levetiracetam 1000 Lacosamide 100	L hippocampal atrophy	L mesial temporal	11/L
P8	M/19	None	Normal	R mesial temporal	11/R
P9	F/50	Lamotrigin 200 Zonisamide 100 Phenobarbital 100	L hippocampal atrophy	L temporal	10/R+6/L
P10	M/32	Levetiracetam 1000 Oxcarbazepin 150	L hippocampal atrophy	L basal temporal	13/L+2/R
P11	M/36	Levetiracetam 1000 Lacosamide 100	L amygdala atrophy	L basal temporal	12/L+2/R
P12	M/37	Carbamazepin 400 Topiramate 200 Clobazam 5	Normal	L perisylvian	13/L
P13	F/23	Carbamazepin 200 Lamotrigin Gabapentin	L hippocampal atrophy	L temporo amygdala	12/L
P14	M/34	Carbamazepin 200 Lamotrigin	L hippocampal atrophy	L mesial temporal and insula	11/L
P15	M/33	Carbamazepin Phenytoin	R frontal dysplasia	R frontal and insula	12/R
P16	F/33	Phenobarbital 100 Topiramate 200	R hippocampal atrophy	R mesial temporal	11/R
P17	F/40	Lamotrigin Valproate Levetiracetam	Parietal malformation	L post parietal	13/L
P18	M/27	Lamotrigin 600 Carbamazepin 600	R frontal dysplasia	R frontal	12/R+2/L
P19	F/18	None	L temporal dysplasia	L parietal	13/L
P20	M/21	Lamotrigin 100 Valproate Pregabalin	R operculo-insula dysplasia	R operculo-insula	12/R
P21	F/51	Oxcarbazepin clobazam	Normal	R temporal	12/R
P22	M/20	Valproate Carbamazepin Levetiracetam	L temporal atrophy	L temporal	13/L
P23	F/31	Valproate 500 Topiramate 10	L temporal dysplasia	L temporal	15/L
P24	M/28	Lamotrigin 400	L frontal & parietal atrophy	L parietal	10/L

TABLE I. (continued).

Patient	Gender/Age	Treatment	MRI	Seizure onset	Number of Electrodes
P25	M/26	Lamotrigin 125 Topiramate 80 Carbamazepin 200	Normal	R hippocampus	13/R
P26	M/36	Levetiracetam 750	R hippocampal atrophy	R temporal	12/R
P27	M/41	Lamotrigin 350 Levetiracetam 1000 Carbamazepin 200	R hippocampal atrophy	R hippocampus	15/R

eliminates the linear enlargement due to X-ray divergence and allows a 1:1 scale so that the films could be used for measurements without any correction. In a second step, the relevant targets were identified on the patient's MRI, previously enlarged to a scale of one-to-one. As MR and angiographic images were at the same scale, they could easily be superimposed, so as to avoid damage to blood vessels and minimize the risk of haemorrhage during electrode implantation.

Anatomical Localization of Electrode Contacts

The localization of the recording contacts was determined using 2 different procedures. In 13 patients implanted before 2010, MRI could not be performed with electrodes in place because of the physical characteristics of the stainless steel contacts. In these cases, the scale 1:1 post implantation skull radiographs performed within the stereotactic frame of Talairach and Tournoux [1988] were superimposed to the pre-implantation scale 1:1 MRI slice corresponding to each electrode track, thus permitting to plot each contact onto the appropriate MRI slice of each patient and determining its coordinates [MRIcro software; Rorden and Brett, 2000]. In the other 14 patients, the implanted electrodes were MRI-compatible and cortical contacts could be directly visualized on the post-operative 3D-MRIs. In both cases, anatomical scans were acquired on a 3-Tesla Siemens Avanto Scanner using a 3D MPRAGE sequence with following parameters: TI/TR/TE 1100/2040/2.95 ms, voxel size: $1 \times 1 \times 1$ mm^3, FOV = 256×256 mm^2.

Intracortical electrode contacts were mapped to the standard stereotaxic space (Montreal Neurological Institute, MNI) by processing MRI data with Statistical Parametric Mapping (SPM12 — Wellcome Department of Cognitive Neurology, UK; http://www.fil.ion.ucl.ac.uk/spm/). Anatomical T1-3D images pre- and post-implantation were co-registered and normalized to the MNI template brain image using a mutual information approach [Maes et al., 1997] and the segmentation module of SPM12, which segments, corrects bias and spatially normalizes images with respect to the MNI model [Ashburner and Friston, 2005]. Then, the cortical localization of electrodes was performed using a regional atlas [WFU Pickatlas v3, Maldjian et al., 2003] in MRIcro®. In the 14 patients with MRI-compatible electrodes, the cortical contacts could be directly visualized on the post-operative normalized 3D-MRIs. In the 13 patients without MRI-compatible electrodes, the coordinates of contacts were determined on their own MRI according to the procedure described above, thus permitting to plot each contact onto the appropriate MRI slice of each patient [MRIcron software; Rorden and Brett, 2000] and determining its MNI coordinates.

Nociceptive-Specific Laser Stimulation

Radiant nociceptive heat pulses of 5 ms duration were delivered with a Nd:YAP-laser (Yttrium Aluminium Perovskite; wavelength 1.34 μm; El.En.®, Florence, Italy). The laser beam was transmitted from the generator to the stimulating probe via an optical fibre of 10 m length (550μm diameter with sub miniature version (SAV) A-905 connector). Perceptive and nociceptive thresholds were determined in each patient immediately before the recording session. Nociceptive thresholds to A-delta stimuli were determined as the minimal laser energy producing a pricking sensation, compared to pulling a hair or receiving a boiling water drop in at least two of three stimuli. They were obtained in all subjects with energy densities between 60 and 100 mJ/mm2 (mean 80 mJ/mm2), which are within the usual data range observed in our laboratory and those reported by others using Nd:YAP lasers [Cruccu et al., 2008]; these parameters have been validated as being able to activate selectively the spinothalamic system in humans [e.g., Garcia-Larrea et al., 2010; Perchet et al., 2012].

Data Acquisition and Recording Procedure

In each patient, two runs of 10–15 stimulations each, at nociceptive threshold, were applied to the skin in the superficial radial nerve territory on the dorsum of the hand contralateral to the hemispheric side of electrodes implantation. The heat spot was slightly shifted over the skin surface between two successive stimuli to avoid both sensitization and peripheral nociceptor fatigue. Fourteen patients were stimulated on the right hand, and thirteen

TABLE II. MNI coordinates (*x*, *y* *z*) of cortical contacts with the largest LEPs

Contacts	P insula ($n = 25$)	A insula ($n = 13$)	P Operc ($n = 8$)	F Operc ($n = 8$)	DLPFC ($n = 13$)	OFC ($n = 7$)	SMA ($n = 7$)	Amygd ($n = 14$)	Hippo ($n = 10$)	PPC ($n = 9$)	Precun ($n = 8$)	pACC ($n = 5$)	ACC ($n = 4$)	MCC ($n = 8$)	dPCC $n = 8$)	vPCC ($n = 5$)
Patients																
P1	37,-20,5							21,-3,-18		52,-48,46	5,-48,46		4,29,22			5,-48,18
P2	37,-24,2							20,-6,-23			8,-55,41					3,-48,23
P3	35,-23,5	33,6,12	61,-26,27		50,22,23 29,46,24	5,46,-14	3,8,57			37,-53,45				4,22,28		4,-50,20
P4	33,-24,5	32,2,8		55,2,8	30,44,11		6,4,52					5,44,14		6,4,36		
P5	35,-23,2	33,11,9	43,-24,23	40,11,9	37,50,9			16,-3,-22								
P6	38,-23,9			45,-9,20					29,-18,-16	43,-58,49				7,17,37		8,-57,25
P7	36,-25,1							21,-9,-26	29,-31,-6		14,-63,45					9,-52,26
P8	35,-22,7	36,11,2	39,-8,17	45,11,3	51,37,21	5,61,-7		25,2,-22	27,-16,-20			7,44,10				
P9	38,-8,-9							21,-7,-18	27,-18,-18							
P10	36,-12,-1					4,54,1		17,0,-11	29,-18,-16						6,-42,31	
P11	39,-5,-4					5,52,1		21,-4,-21	24,-15,-16							
P12	37,-12,2	35,8,5	46,-5,17		42,48,9	7,48,-11		24,-2,-21				8,46,7				
P13	35,-12,17	34,8,9												2,2,32	8,-28,39	
P14	33,-24,6	36,2,-3							22,-10,-23							
P15	33,-7,13	33,7,11			51,45,5	9,61,19	8,19,48					5,39,2				
P16	32,-21,12			41,-4,14												
P17	37,-3,-4										9,-57,47				6,-48,33	
P18		33,24,6		44,5,10	52,32,19	6,41,-13	5,3,70				5,-51,52		5,32,18	7,-7,38		
P19	38,-2,-5	34,-4,11		52,-4,11	49,20,34		6,0,64		24,-1,-28		8,-66,44			4,20,34	2,-30,33	
P20	38,-6,4	35,9,10	57,0,16	49,9,10	46,32,23		5,0,71	15,-2,-19		61,-37,44			4,32,23	5,-10,37		
P21	37,-1,-4	38,16,1	49,-3,18					15,-6,-20	22,-15,-25						10,-45,25	
P22	38,-16,17	35,0,11	55,0,11		38,41,6		9,12,51	18,-3,-20								
P23	42,-29,9				39,51,9				24,-13,-16	46,-45,50 45,-45,36	6,-43,46		6,30,20	7,-10,48	7,-43,34	
P24										39,-43,54	10,-43,55					
P25	36,-17,19		44,-17,20							57,-45,36					7,-43,33	
P26	39,-19,2				37,54,15			26,-3,-17								
P27	41,-8,-12							20,-6,-17		60,-44,31		8,40,8			9,-40,31	
Mean	37,-15,5	34,8,7	49,-10,19	46,3,11	42,40,16	6,52,-3	6,7,59	20,-4,-20	26,-16,-18	49,-46,43	8,-53,47	7,43,8	5,31,21	5,5,36	8,-40,32	6,-51,22
SD	2,9,7	2,7,5	8,11,5	5,8,5	8,11,9	2,8,12	2,7,9	4,3,4	3,8,6	9,6,8	3,9,4	2,3,4	1,2,2	2,13,6	2,7,4	3,4,3

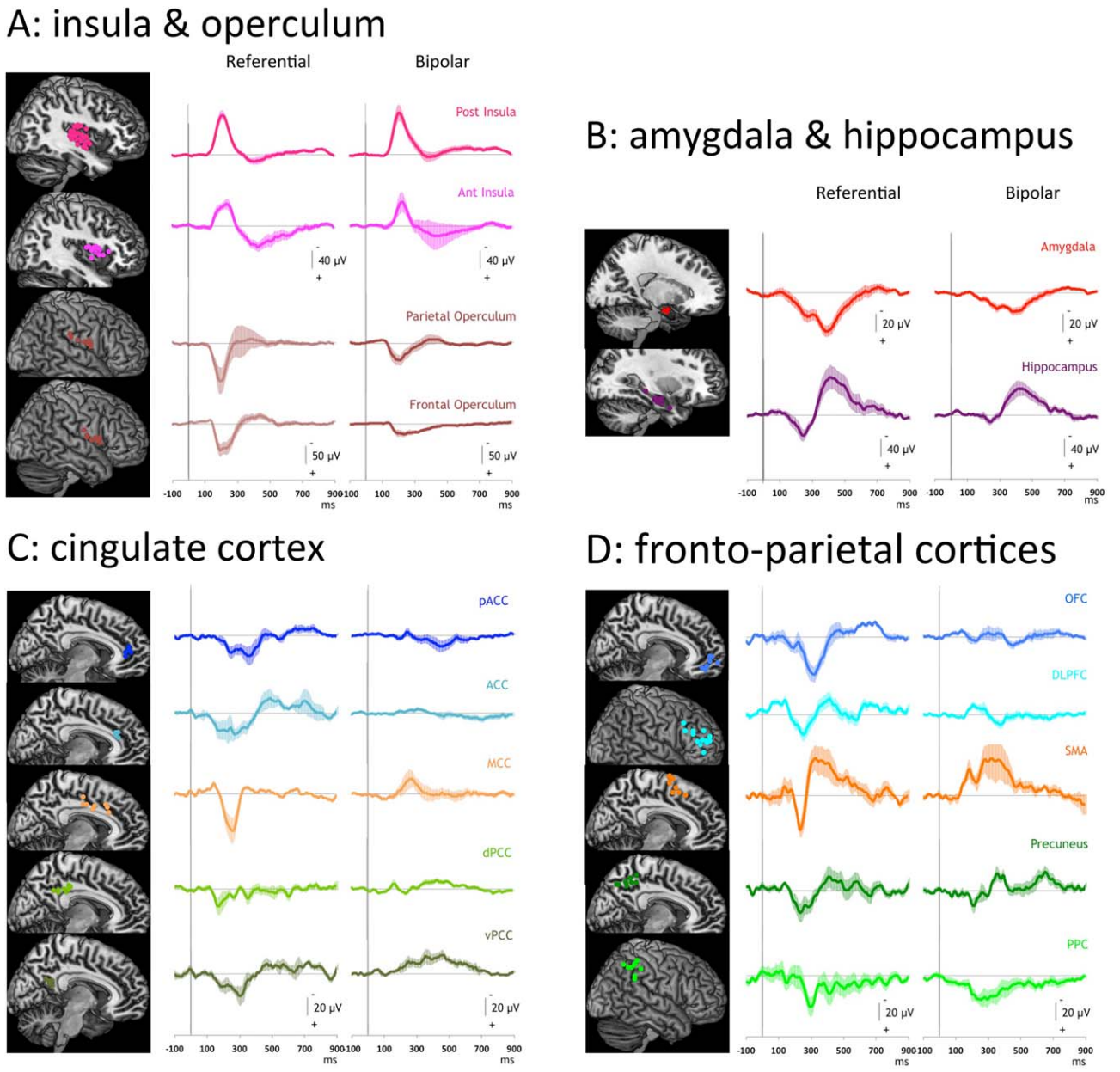

Figure 1.

Laser evoked potentials recorded in the 16 studied areas. **A**: Responses obtained in posterior ($n = 25$) and anterior ($n = 13$) insulae, parietal ($n = 8$) and frontal ($n = 8$) operculi. **B**: Responses obtained in amygdala ($n = 14$) and hippocampus ($n = 10$). **C**: Responses obtained in cingulate cortices: pACC ($n = 5$), ACC ($n = 4$), MCC ($n = 8$), dPCC ($n = 8$), vPCC ($n = 5$). **D**: Responses obtained in OFC ($n = 7$), DLPFC ($n = 13$), SMA ($n = 7$), precuneus ($n = 8$)and PPC ($n = 9$). For each area Left: Recording contact locations in each area represented on MNI Brain templates; Right: Grand averages (+/- SEM) of responses obtained in each area (in referential and bipolar modes).

on the left hand. Recordings were performed in common referential mode, the reference electrode being chosen for each patient on an implanted contact located in the skull. EEG was recorded continuously at a sampling frequency of 256 Hz or 512 Hz from 96 to 128 channels, amplified and band pass filtered (0.33 − 128 Hz; −3dB, 12 dB/octave) to be stored in hard disk for off-line analysis (Micromed SAS®, Macon France).

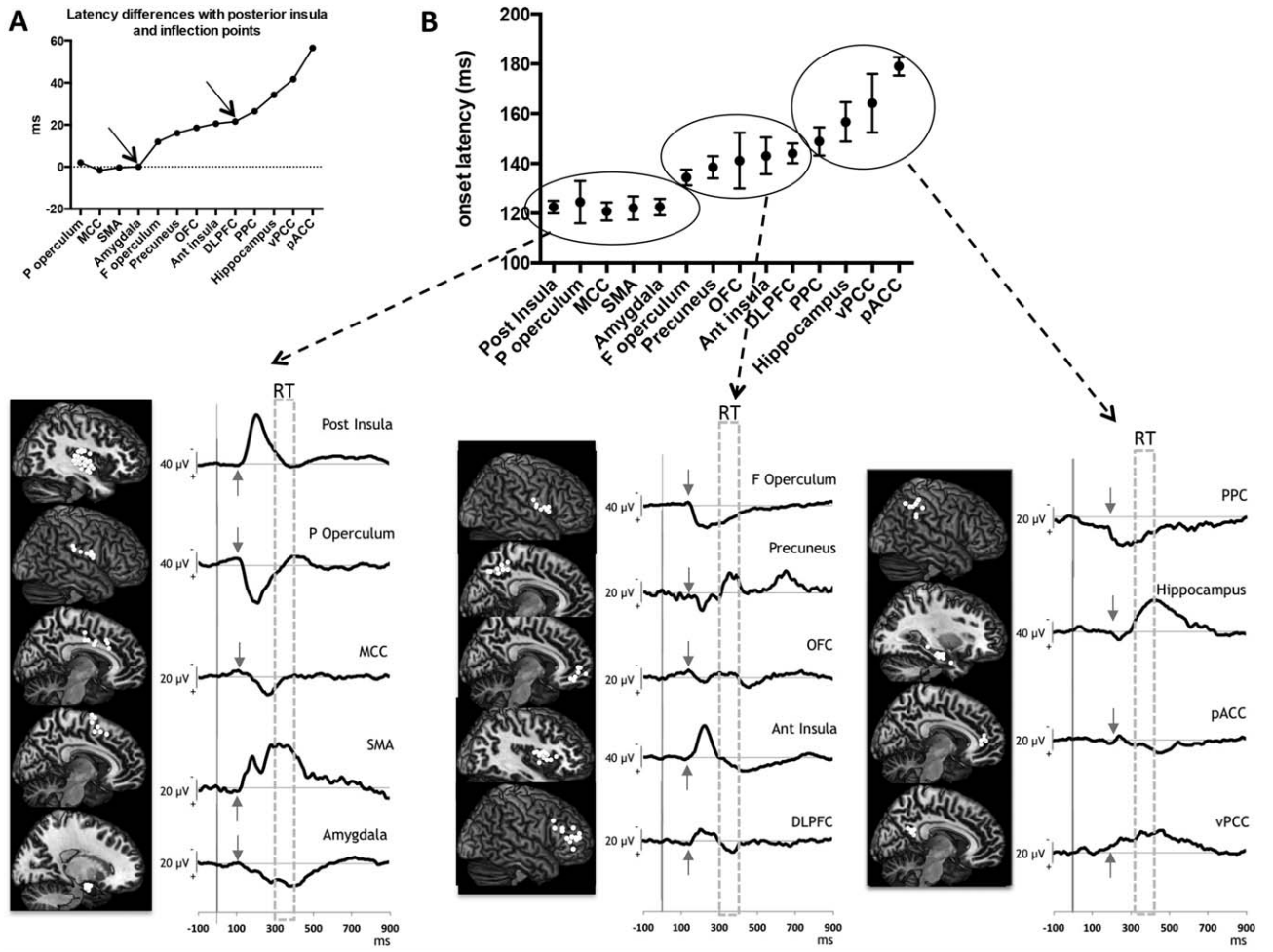

Figure 2.

Onset latencies of the nociceptive responses recorded in the 14 areas analyzed (bipolar mode). **A**: Latency differences between the 13 areas, relative to that of the posterior insula. Two points of inflection clearly distinguish 3 groups: the first one with virtually no latency difference relative to the post-insula comprising the parietal operculum, mid cingulate, SMA, and amygdala (latency difference around zero); the second group with a progressive but relatively small latency increase including the frontal operculum, anterior insula, precuneus, OFC, DLPFC, and the third group with a greater rate of latency increase including the posterior parietal cortex, posterior and perigenual cingulate, and hippocampus. **B**: Onset latencies (top) and grand-averaged traces (bottom) of the three groups: the first one with a 110 − 130 ms onset latency range; the second with a 130 − 150 ms onset latency range and the third one with a 150 − 180 ms onset latency range. The small arrows point to the mean onset of the responses and the areas delineated with dotted lines correspond to time windows during which motor reaction occurred (RT).

ELECTROPHYSIOLOGICAL DATA ANALYSES

Motor Reaction Times

Motor reaction times were calculated in 10 patients using synchronized EEG and video signals, both simultaneously digitized at 256 or 512 Hz. Video recordings being available in every room, this technique was preferred to EMG which would have imposed to place extra-electrodes. The onset latency of the finger lift in response to the stimulus was regarded as a correlate of stimulus conscious perception.

Laser-Evoked Potentials (LEPs)

The coordinates of the contacts exhibiting the largest responses to laser stimuli are indicated on Table II. Epoching of the EEG, selective averaging, and recordings analyses were performed off-line using BrainVision® System

(Brain Products®, Munich, Germany). Epochs presenting contamination by epileptic transient activities or artefacts exceeding 250 μV were rejected from analysis, the rate of rejection being of ~10%. LEP components recorded in the different structures were assessed using both monopolar (referential) and bipolar montages (with adjacent contact), within a time window of 100 ms pre- and 900 ms post-stimulus. The consistency of responses from each area was estimated as the percentage of patients in whom a reproducible response could be obtained from that area. Consistency of responses was estimated by superimposing the EPs to two consecutive runs of stimuli (or the responses to "odd" and "even" stimuli within a single long run). Responses from a given region were considered for analysis only when they were of higher amplitude than the mean baseline value ± 3 SD in at least 70% of the single trials. Then, responses from same regions in different patients were also superimposed to assess between-subject reproducibility, inter-subject variability being quantified by the point-by-point standard errors (SEM) on grand averages. In bipolar montages, were measured in each patient: (1) the onset and peak latencies of the LEP main component, and (2) its amplitude (from onset to peak). Onsets were defined at the inflection point when amplitude values of the signal differed by two standard deviations from the mean pre-stimulus baseline. Statistical analyses were performed with GraphPad Prism 6 and StatView® softwares. Latencies and amplitudes were submitted to one-way ANOVA with cortical areas as between factor, and significance level set at $P < 0.05$ (Greenhouse-Geisser corrected if needed). Pre-defined contrast or post-hoc tests (Holm-Sidak test corrected for multiple comparisons) were applied in case of significant effects following ANOVA.

Insular-Cortical Coherence

Functional connectivity was studied using EEG phase-coherence analysis with the posterior insular region as "seed region" with respect to the rest of the cortical areas analyzed (MNI coordinates indicated in Table II). The posterior insula was chosen as the principal "seed" area, since it receives the earliest nociceptive signal [Frot et al., 1999; Lenz et al., 1998b] and the most important sensory projections from the spinothalamic system (STS) [Dum et al., 2009]. Phase coherence was computed within three time windows: 100 − 400 ms, 400 − 700 ms, and 700 − 1000 ms following each nociceptive stimulus, after Fast Fourier Transform of the signal for each spectral band power (delta: 1 − 3 Hz, theta: 4 − 7 Hz, alpha: 8 − 12 Hz, beta: 13 − 29 Hz, gamma: 30 − 64 Hz). The first time window was chosen according to previous data obtained with intracerebral recordings showing that the operculo-insular LEPs are recorded within these latency borders [Frot et al., 1999, 2014; Lenz et al., 1998; Ohara et al., 2004]. The two other time windows were defined so as to divide the post-stimulus period in two equivalent epochs (300 ms each). The phase coherence was calculated as the quotient between correlation and autocorrelation for each frequency and each channel pair, and underwent Fisher's z-transformation before statistical analysis. Individual coherence values between posterior insula and the different cortical areas were submitted to a three-way mixed ANOVA with "Frequency band" and "Time window" as within factors, and "Cortical area" as between factor. Post-hoc tests (Holm-Sidak test corrected for multiple comparisons) were applied in case of significant effects following ANOVA.

RESULTS

Behavioral Data

All the patients described a "pricking" sensation associated to the laser stimulus. Mean motor reaction times (index lift) indicating stimulus detection were recorded at 349 ± 58 ms after stimulus onset (median: 368.33 ms; range: 260 − 422 ms).

Timing and Amplitude of Cortical Nociceptive Responses

Grand averages of responses from the 16 cortical areas analyzed are illustrated in Figure 1. On bipolar montages, local field responses to nociceptive laser pulses were systematically obtained (100% of cases) in the posterior and anterior insulae, parietal and frontal opercula, mid-cingulate cortex (MCC), supplementary motor area (SMA), amygdala, hippocampus, orbitofrontal cortex (OFC), and postero-inferior parietal cortex (PPC, BA40). Responses were fairly systematic in the precuneus (88%), the perigenual and ventral posterior cingulate (pACC and vPCC; 80%), and the dorsolateral prefrontal cortices (DLPFC; 62%), while their incidence dropped to 50% in the anterior cingulate cortex (ACC), and 36% in the dorsal posterior cingulate (dPCC). Due to their inconstant presence across our subjects, the responses obtained in ACC and dPCC were not further included in statistical analyses.

One-way ANOVA demonstrated a highly significant inhomogeneity of onset latencies across regions [$F(13, 126) = 7.673$; $P < 0.0001$]. Latency discontinuities were assessed by determining the differences between successive latencies, relative to that of the posterior insula. The graph (Fig. 2A) shows two points of inflection: first, there is virtually no latency difference with respect to the posterior insula in the parietal operculum, mid cingulate, SMA and amygdala; then, a progressive latency increase is observed for all the other structures, with, initially, a relatively small latency increase of 12-20 ms in 5 structures (frontal operculum, anterior insula, precuneus, OFC, DLPFC), followed by a greater rate of latency increase (26–56 ms) in 4 other regions (posterior parietal, posterior, and perigenual cingulate, and hippocampus). Predefined contrast analyses showed significant differences between the three groups: the first group had shorter latencies

TABLE III. Values ± SEM of the onsets latencies, peak latencies, and peak amplitudes of the responses in the different cortical areas

	Onset latency (ms)	Highest peak latency (ms)	Highest peak amplitude (μV)
Posterior insula	122.5 ± 2.5	210.2 ± 4.1	80 ± 12.2
Parietal operculum	124,5 ± 8.5	189.6 ± 11.5	92.4 ± 15.8
MCC	120.8 ± 3.6	241.8 ± 3.7	37.3 ± 9.4
SMA	122.1 ± 4.7	183.7 ± 6.1	28 ± 10.2
Amygdala	122.5 ± 3.3	407.6 ± 9.7	38.1 ± 3.4
Frontal operculum	134.4 ± 3.2	228.8 ± 15.6	50.8 ± 9.9
Precuneus	138.5 ± 4.5	350 ± 3.8	29.5 ± 10.4
OFC	141.1 ± 11.2	318.7 ± 22.9	17 ± 3.1
Anterior insula	143.1 ± 7.4	239.9 ± 8.9	57.1 ± 18.7
DLPFC	144.1 ± 4	226.3 ± 9	22.7 ± 4.2
PPC	148.9 ± 5.7	273 ± 7.5	27.6 ± 6.1
Hippocampus	156.7 ± 7.9	411.1 ± 10.7	63.6 ± 12.4
vPCC	164.2 ± 11.8	349.8 ± 6.9	25 ± 6.2
pACC	179 ± 3.7	398.4 ± 17.9	17.4 ± 5.2

relative to the second and third groups ($F = 23.31$, $P < 0.0001$ and $F = 84.06$, $P < 0.0001$ respectively) and the second group shorter than the third one ($F = 24,98$, $P < 0.0001$) (Fig. 2B and Table III).

ANOVA on the latency of the highest peak of the response also showed a significant effect of cortical areas [F (13, 126) = 72.19; $P < 0.0001$], peak latency being delayed in the amygdala, hippocampus, pACC, vPCC, PPC, precuneus, and OFC (near 400 ms) as compared to the posterior and anterior insulae, the parietal and frontal operculi, and SMA (Table III). Amplitudes of the highest peak were also significantly different according to the cortical areas [$F(13,126) = 3.83$; $P < 0.0001$]. Although mean amplitudes were higher in posterior insula and parietal operculum relative to all other areas, after correction for multiple comparisons differences reached significance when compared with DLPFC and OFC.

Functional Connectivity (Spectral Coherence) Analyses

Since the posterior insula receives the most important spinothalamic projections in primates [Dum et al., 2009], coherence analysis was performed using this structure as "seed" for all other brain regions. On these conditions, a three-way ANOVA on spectral coherence values (factors: cortical area, time window and frequency band) showed a significant effect of cortical area [$F(12,96) = 2.613$; $P = 0.0047$] and time window [$F(2,24) = 5.736$; $P = 0.0038$], with no effect of frequency spectral band and no interaction (Fig. 3A).

Coherence values cumulated across bands increased significantly between the first time-window (100 − 400 ms), and the two others (400 − 700 ms and 700 − 1,000 ms); ($t(544) = 4.81$; $P < 0.0001$; and $t(544) = 3.64$; $P = 0.0006$) (Fig. 3B). Coherence levels with the posterior insula increased with time in a large majority of other cortical areas (Fig. 4) Irrespective of time-window, the largest spectral coherence values with the posterior insula were observed in the anterior insula, parietal operculum, and pACC (Figs. 3C and 4).

DISCUSSION

To the best of our knowledge, this is the first time that intracortical human recordings from such a diversity of cortical areas have been gathered in response to nociceptive-specific activation. Many of the areas studied here pertain to the classical network activated by painful stimuli in functional imaging studies, while others, including the amygdala, hippocampus and posterior cingulate, are seldom reported. Altogether our results provide evidence for parallel and simultaneous initial nociceptive input to sensory, motor, and one limbic region (the amygdala) through spinothalamic and extra-thalamic ascending pathways. This initial stage is followed by a relatively ordered activation of different groups of cortical structures, which may lead from unconscious nociceptive processing to conscious perception, self-awareness, and memory encoding.

Parallel Responses in Sensory, Motor and Limbic Areas

Five regions responded with earliest latencies to nociceptive input: two were sensory cortices (posterior insula, parietal operculum), two were motor regions (SMA, midcingulate) and one was a limbic structure (amygdala). These regions were activated with very similar onset latencies of 110 − 120 ms (Fig. 2), thus providing physiological evidence that nociceptive input can simultaneously trigger sensory, motor, and limbic responses in the human brain. While the temporal coincidence of sensory and motor-cingulate EEG responses has already been shown [Frot et al., 2008, 2013; Ohara et al., 2004, 2006], activation of the

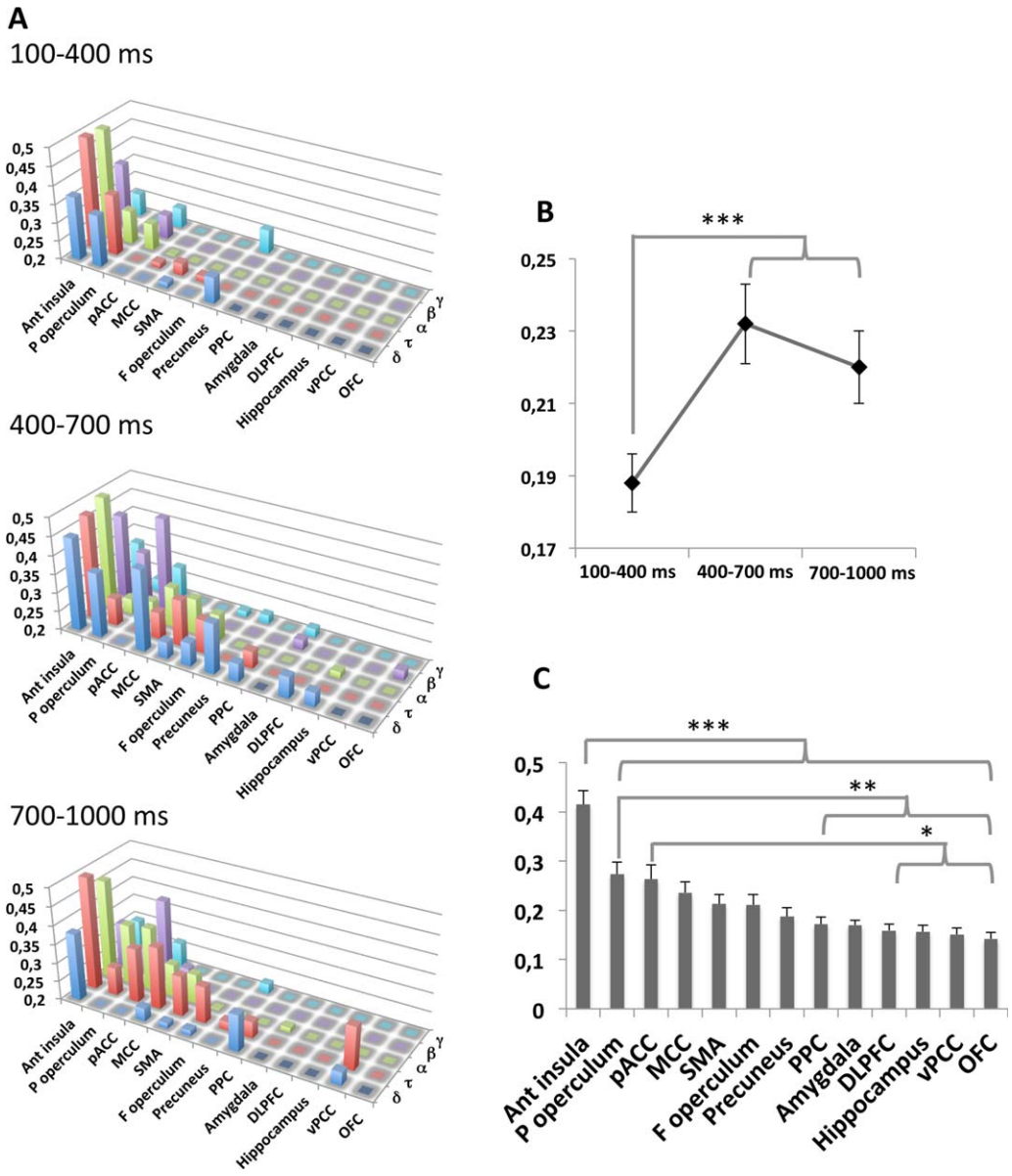

Figure 3.

A: Phase coherence level of EEG frequency bands between posterior insula and the 13 cortical structures calculated in the 100 − 400 ms, 400 − 700 ms, and 700 − 1,000 ms time windows following nociceptive stimuli. Ordinate: level of coherence from 0.2 to 0.5; abscissa: cortical structures (anterior insula, parietal operculum, pACC, MCC, SMA, frontal operculum, precuneus, PPC, amygdala, DLPFC, hippocampus, vPCC, OFC); third coordinate: frequency bands (δ, τ, α, β, γ). **B**: Mean levels of coherence between posterior insula and all other areas according to time window, showing the significant increase of this level during the second and third time window as compared to the first one. **C**: Mean levels of coherence between posterior insula and each of the other areas, showing highest values for the anterior insula, parietal operculum, and pACC as compared to the others.

limbic cortex has been typically considered to follow sensory activation, rather than being concomitant to it [Inui et al., 2003; Kakigi et al., 2004]. Human amygdalar recordings to noxious stimuli have been scarce so far, and showed either long latency responses [Liu et al., 2010, Moont et al., 2011] or no response at all [Frot et al., 1999]. Figure 2 in Liu et al. [2010], however, shows that at least in one subject amygdalar responses developed at latencies

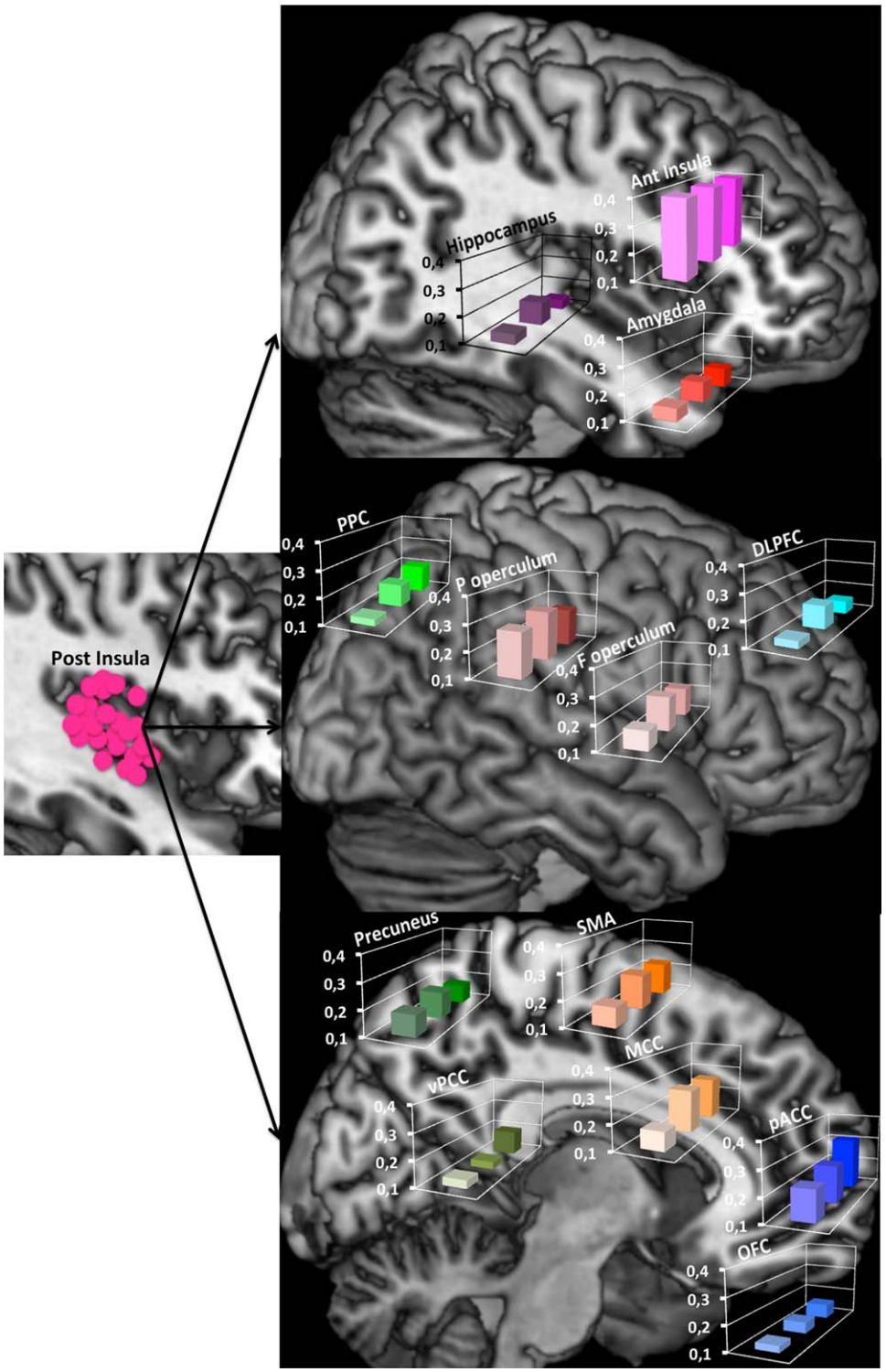

Figure 4.

Phase spectral coherences during the three time windows represented on normalized anatomical model of the brain proposed by the McConnell Brain Imaging Centre of the Montreal Neurological Institute. Coherences between posterior insula and 13 cortical areas: Left. Recording contact locations in the posterior insula represented on a sagittal slice. Top: Sagittal slice for anterior insula, amygdala and hippocampus; Mid: Brain convexity for posterior parietal cortex, parietal operculum, frontal operculum and dorso-lateral prefrontal cortex; Bottom. Mid-sagittal slice for precuneus, ventral posterior cingulate, SMA, mid cingulate, perigenual anterior cingulate and orbito-frontal cortex. Levels of coherence during the three time windows are represented in each histogram. Ordinate: level of coherence from 0.1 to 0.4; abscissa: time windows (front: 100 – 400, middle: 400 – 700, back: 700 – 1,000 ms). Note that the coherence values between the insula and a large majority of other cortical areas increase with time.

consistent with those in the present work, and early onset gamma oscillations in the amygdala have been also recently described in response to fearful faces [review Sato et al., 2013].

The presence of early-onset amygdalar nociceptive responses in this study is consistent with anatomo-physiological data in mammals, from rodents to primates. Spinal fibres carrying noxious stimuli from the spinal cord project heavily onto neurons in the pontine parabrachial nucleus, which in turn send monosynaptic projections toward the amygdalar body ensuring a di-synaptic nociceptive route [Bernard and Besson, 1988; Gauriau and Bernard, 2002]. Transneuronal labelling indicates that such spino–parabrachial–amygdalar connection represents a functional pathway [Dum et al., 2009; Jasmin et al., 1997; review Veinante et al., 2013]; in particular, injection of herpes virus in the dorsal horn of macaques infected neurons in the central amygdala with identical timing as those in the posterior insula [Dum et al., 2009], demonstrating that the spino-amygdalar primate pathway is functional and disynaptic. It can be reasonably concluded that amygdala responses to laser stimuli were, at least in their early phase, generated through such a rapid route.

Amygdalar potentials had slower slope and longer duration than the rest of early-onset responses. Nociceptive information can reach this structure not only via the rapid spino-parabrachial route, but also through pathways involving three or more relays, via brainstem nuclei, intralaminar thalamus and anterior insula [Friedman et al., 1986; Mesulam et al., 1982; Nieuwenhuys 2012; Veinante et al., 2013]. Our results suggest a cumulative nociceptive input to the amygdala, and this may be relevant in the context of hypotheses suggesting that the role of amygdala in emotional judgment might emerge from the convergence of inputs issued from multiple areas [Omigie et al., 2015].

The Construction of "Pain Awareness"

Motor reaction times (RTs) to the laser pulses are an indirect indication of stimulus awareness. Their mean onset in our subjects was 349 ± 58 ms, and the earliest single reactions developed around 260 ms. These latencies are earlier than those reported when responding via a button press [Dusch et al., 2016] and comparable to those obtained via EMG recordings in healthy subjects [Perchet et al., 2012]. Activation of posterior operculo-insular cortex, motor cingulate and amygdala preceded by more than 120 ms the earliest motor reaction, and was therefore likely to be initiated prior to conscious awareness. Indeed, neural activity limited to sensory areas cannot ensure conscious perception [Aru et al., 2012; Del Cul et al., 2007; Rees et al., 2000], even when limbic regions are co-activated [Troiani et al., 2014; Vuilleumier et al., 2002], and conscious awareness requires joint activation of multiple networks including prefrontal and parietal areas [Beck et al., 2001; Haynes et al., 2005; Pessoa, 2008]. In our subjects, prefrontal, posterior parietal, and anterior insular regions became activated later than sensori-motor and limbic areas, and remained active until at least 500 ms post-stimulus. Hence, an ensemble of sensorimotor, limbic, and fronto-parietal structures was simultaneously active during the 250–400 ms window, when conscious awareness of the stimulus was likely to emerge (Fig. 2). Data from other sensory systems indicate that declarative awareness only occurs when activation of fronto-parietal networks adds up to that of sensory cortices, hence making information available to high-level processes including intentional action [Dehaene et. al 1989; Del Cul et al., 2007]. Access to consciousness has been shown to concur with an increase in functional correlation between stimulus-specific areas and high-order frontal networks [Dehaene et al., 2001; Gross et al., 2004; Haynes et al., 2005], and such increase in coupling was also observed here, with progressive enhancement of spectral coherence between parieto-frontal regions and the sensory posterior insula (Fig. 3). Of notice, the connectivity pattern in the 200–500 ms post-stimulus period was strikingly similar to that reported during the emergence of consciousness from anesthesia [Långsjö et al., 2012]. In each case, activation of a core network of sensory and limbic regions functionally coupled with parts of frontal and inferior parietal cortices appears as an important concomitant, perhaps a determinant, of the access of the stimulus to conscious awareness.

The last group of cortical regions to become activated comprised the hippocampal formation and the two extreme segments of the cingulate, respectively around the genu (perigenual cingulate, pACC) and the splenium of the corpus callosum (ventral posterior cingulate, vPCC). These two regions share a role in what has been termed "internal awareness" [see Demertzi et al., 2013; Fig. 1) but their function in the context of pain appear different. Perigenual responses tend to be enhanced during hyperalgesia, either induced pharmacologically [Lorenz and Casey, 2005; Schweinhardt et al., 2006] or through observation of pain in others [Godinho et al., 2012], and have been interpreted as reflecting a link between pain awareness and triggering of descending pain controls [Garcia-Larrea and Peyron, 2013]. This is supported by the co-activation of perigenual areas and descending modulatory regions such as the periaqueductal grey [An et al., 1998; Kupers et al., 2004; Zambreanu et al., 2005], and also the fact that perigenual responses, most often deficient in neuropathic pain, can be restored by analgesic procedures that also enhance descending inhibition [Garcia-Larrea and Peyron, 2013; Peyron et al., 2007; Willoch et al., 2003]. In contrast, the ventral perisplenial cingulate (v-PCC) is rather considered to sustain processes involved in self-monitoring, participate to the interface between external world and the sense of the self [Gusnard et al., 2001], and be involved in the network sustaining self-referential processing (reviews in Vogt 2005; Brewer et al., 2013; Demertzi et al., 2013;

DeWitt et al., 2015]. Such functional dissimilarities between perigenual and perisplenial cingulate are sustained by differences in connectivity patterns: the extensive subcortical connections of the perigenual are lacking in the posterior ventral cingulate [Vogt, 2005], which in turn is connected with cortical areas, prominently including memory-supporting regions such as the hippocampal formation [Bzdok et al., 2015; Kobayashi and Amaral, 2007; Parvizi et al., 2006]. The belated activation of these regions in our subjects, as well as the late increase in functional coherence between them and the posterior insular cortex (Fig. 3A) support their role in high-level stages of stimulus processing, linking up external and internal sensory worlds. Of notice, "external" and "internal awareness" networks appear functionally disconnected in altered states of consciousness such as vegetative state [Demertzi et al., 2013], suggesting the inability of these patients to fully map noxious stimuli onto declarative consciousness.

Limitations of the Study

The present work analyzed cortical responses using nociceptive stimuli exclusively, without control from non-noxious stimuli. Response latencies, in the 100–400 ms range, are however exclusively compatible with the timing of activation of the STT, as the dorsal-column system gives rise to much earlier responses ($15-20$ ms) [Allison et al., 1989; Bradley et al., 2016]. Also, functional links through phase-coherence analysis do not prove causal influences from one structure over another, and may result from functional connections through intermediary regions not recorded here [Liu et al., 2011]. Finally, the data presented here, although extensive, could not provide a full view of all cortical regions responding to noxious input during the first second; in particular, many areas of the temporal lobe were lacking, due to their frequent involvement in the epileptic process.

CONCLUSION

Our data suggest that human cortical nociceptive processing is initiated simultaneously in sensory, motor and limbic areas; it progresses in less than one second to the recruitment of fronto-parietal and anterior insular networks, and finally to the activation of perigenual, posterior cingulate and hippocampal structures. Functional connectivity (spectral coherence) between sensory and high-level networks increases progressively during the first second, in accordance with other studies on sensory awareness.

REFERENCES

Allison T, McCarthy G, Wood CC, Darcey TM, Spencer DD, Williamson PD (1989): Human cortical potentials evoked by stimulation of the median nerve. I. Cytoarchitectonic areas generating short-latency activity. J Neurophysiol 62:694–710.

An X, Bandler R, Ongür D, Price JL (1998): Prefrontal cortical projections to longitudinal columns in the midbrain periaqueductal gray in macaque monkeys. J Comp Neurol 401:455–479.

Apkarian AV, Bushnell MC, Treede RD, Zubieta JK (2005): Human brain mechanisms of pain perception and regulation in health and disease. Eur J Pain 9:463–484.

Aru J, Axmacher N, Do Lam AT, Fell J, Elger CE, Singer W, Melloni L (2012): Local category-specific gamma band responses in the visual cortex do not reflect conscious perception. J Neurosci 32:14909–14914.

Ashburner J, Friston KJ (2005): Unified segmentation. Neuroimage 26:839–851.

Bastuji H, Frot M, Mazza S, Perchet C, Magnin M, Garcia-Larrea L (2015): Thalamic responses to nociceptive-specific input in humans: Functional dichotomies and thalamo-cortical connectivity. Cereb Cortex doi: 10.1093/cercor/bhv106.

Beck DM, Rees G, Frith CD, Lavie N (2001): Neural correlates of change detection and change blindness. Nat Neurosci 4: 645–650.

Bernard JF, Besson JM (1988): Convergence of nociceptive information on the parabrachio-amygdala neurons in the rat. C R Acad Sci III 307:841–847.

Bradley C, Joyce N, Garcia-Larrea L (2016): Adaptation in human somatosensory cortex as a model of sensory memory construction: A study using high-density EEG. Brain Struct Funct 221: 421–431.

Brewer JA, Garrison KA, Whitfield-Gabrieli S (2013): What about the "Self" is Processed in the Posterior Cingulate Cortex? Front Hum Neurosci 7:647.

Buckner RL (1998): Event-related fMRI and the hemodynamic response. Hum Brain Mapp 6:373–377.

Bzdok D, Heeger A, Langner R, Laird AR, Fox PT, Palomero-Gallagher N, Vogt BA, Zilles K, Eickhoff SB (2015): Subspecialization in the human posterior medial cortex. Neuroimage 106: 55–71.

Cappe C, Morel A, Barone P, Rouiller EM (2009): The thalamocortical projection systems in primate: An anatomical support for multisensory and sensorimotor interplay. Cereb Cortex 19: 2025–2037.

Cruccu G, Aminoff MJ, Curio G, Guerit JM, Kakigi R, Mauguiere F, Rossini PM, Treede RD, Garcia-Larrea L (2008): Recommendations for the clinical use of somatosensory-evoked potentials. Clin Neurophysiol 119:1705–1719.

Dehaene S, Naccache L (2001): Towards a cognitive neuroscience of consciousness: Basic evidence and a workspace framework. Cognition 79:1–37.

Dehaene S, Changeux JP, Naccache L, Sackur J, Sergent C (2006): Conscious, preconscious, and subliminal processing: A testable taxonomy. Trends Cogn Sci 10:204–211.

Del Cul A, Baillet S, Dehaene S (2007): Brain dynamics underlying the nonlinear threshold for access to consciousness. PLoS Biol 5:e260.

Demertzi A, Soddu A, Laureys S (2013): Consciousness supporting networks. Curr Opin Neurobiol 23:239–244.

DeWitt SJ, Ketcherside A, McQueeny TM, Dunlop JP, Filbey FM (2015): The hyper-sentient addict: an exteroception model of addiction. Am J Drug Alcohol Abuse 41:374–381.

Dum RP, Levinthal DJ, Strick PL (2009): The spinothalamic system targets motor and sensory areas in the cerebral cortex of monkeys. J Neurosci 29:14223–14235.

Dusch M, van der Ham J, Weinkauf B, Benrath J, Rukwied R, Ringkamp M, Schmelz M, Treede RD, Baumgärtner U (2016): Laser-evoked potentials mediated by mechano-insensitive nociceptors in human skin. Eur J Pain 20: 845–854.

Friedman DP, Murray EA, O'Neill JB, Mishkin M (1986): Cortical connections of the somatosensory fields of the lateral sulcus of macaques: Evidence for a corticolimbic pathway for touch. J Compar Neurol 252:323–347.

Frot M, Rambaud L, Guenot M, Mauguiere F (1999): Intracortical recordings of early pain-related CO2-laser evoked potentials in the human second somatosensory (SII) area. Clin Neurophysiol 110:133–145.

Frot M, Mauguière F, Magnin M, Garcia-Larrea L (2008): Parallel processing of nociceptive A-delta inputs in SII and midcingulate cortex in humans. J Neurosci 28:944–952.

Frot M, Magnin M, Mauguière F, Garcia-Larrea L (2013): Cortical representation of pain in primary sensory-motor areas (S1/M1)-a study using intracortical recordings in humans. Hum Brain Mapp 34:2655–2668.

Frot M, Faillenot I, Mauguière F (2014): Processing of nociceptive input from posterior to anterior insula in humans. Hum Brain Mapp 35:5486–5499.

Garcia-Larrea L, Perchet C, Creac'h C, Convers P, Peyron R, Laurent B, Mauguière F, Magnin M (2010): Operculo-insular pain (parasylvian pain): A distinct central pain syndrome. Brain 133:2528–2539.

Garcia-Larrea L, Peyron R (2013): Pain matrices and neuropathic pain matrices: A review. Pain 154:S29–S43.

Gauriau C, Bernard JF (2002): Pain pathways and parabrachial circuits in the rat. Exp Physiol 87:251–258.

Godinho F, Faillenot I, Perchet C, Frot M, Magnin M, Garcia-Larrea L (2012): How the pain of others enhances our pain: Searching the cerebral correlates of 'compassional Hyperalgesia'. Eur J Pain 16:748–759.

Gross J, Schmitz F, Schnitzler I, Kessler K, Shapiro K, Hommel B, Schnitzler A (2004): Modulation of long-range neural synchrony reflects temporal limitations of visual attention in humans. Proc Natl Acad Sci USA 101:13050–13055.

Guenot M, Isnard J, Ryvlin P, Fischer C, Ostrowsky K, Mauguiere F, Sindou M (2001): Neurophysiological monitoring for epilepsy surgery: The Talairach SEEG method. StereoElectroEncephaloGraphy. Indications, results, Complications and therapeutic applications in a series of 100 consecutive cases. Stereotact Funct Neurosurg 77:29–32.

Gusnard DA, Akbudak E, Shulman GL, Raichle ME (2001): Medial prefrontal cortex and self-referential mental activity: Relation to a default mode of brain function. Proc Natl Acad Sci USA 98:4259–4264.

Haynes JD, Driver J, Rees G (2005): Visibility reflects dynamic changes of effective connectivity between V1 and fusiform cortex. Neuron 46:811–821.

Inui K, Tran TD, Qiu Y, Wang X, Hoshiyama M, Kakigi R (2003): A comparative magnetoencephalographic study of cortical activations evoked by noxious and innocuous somatosensory stimulations. Neuroscience 120:235–248.

Jasmin L, Burkey AR, Card JP, Basbaum AI (1997): Transneuronal labeling of a nociceptive pathway, the spino-(trigemino-)parabrachio-amygdaloid, in the rat. J Neurosci 17: 3751–3765.

Kakigi R, Inui K, Tran DT, Qiu Y, Wang X, Watanabe S, Hoshiyama M (2004): Human brain processing and central mechanisms of pain as observed by electro- and magnetoencephalography. J Chin Med Assoc 67:377–386.

Kobayashi Y, Amaral DG (2007): Macaque monkey retrosplenial cortex. III. Cortical efferents. J Comp Neurol 502:810–833.

Kupers R, Faymonville ME, Laureys S (2005): The cognitive modulation of pain: Hypnosis- and placebo-induced analgesia. Prog Brain Res 150:251–269.

Långsjö JW, Alkire MT, Kaskinoro K, Hayama H, Maksimow A, Kaisti KK, Aalto S, Aantaa R, Jääskeläinen SK, Revonsuo A, Scheinin H (2012): Returning from oblivion: Imaging the neural core of consciousness. J Neurosci 32:4935–4943.

Legrain V, Perchet C, García-Larrea L (2009): Involuntary orienting of attention to nociceptive events: neural and behavioral signatures. J Neurophysiol 102:2423–2434.

Lenz FA, Rios M, Zirh A, Chau D, Krauss G, Lesser RP (1998a): Painful stimuli evoke potentials recorded over the human anterior cingulate gyrus. J Neurophysiol 79:2231–2234.

Lenz FA, Rios M, Chau D, Krauss GL, Zirh TA, Lesser RP (1998b): Painful stimuli evoke potentials recorded from the parasylvian cortex in humans. J Neurophysiol 80:2077–2088.

Liu CC, Ohara S, Franaszczuk PJ, Zagzoog N, Gallagher M, Lenz FA (2010): Painful stimuli evoke potentials recorded from the medial temporal lobe in humans. Neuroscience 165:1402–1411.

Liu CC, Shi CQ, Franaszczuk PJ, Crone NE, Schretlen D, Ohara S, Lenz FA (2011): Painful laser stimuli induce directed functional interactions within and between the human amygdala and hippocampus. Neuroscience 178:208–217.

Lorenz J, Casey KL (2005): Imaging of acute versus pathological pain in humans. Eur J Pain 9:163–165.

Maes F, Collignon A, Vandermeulen D, Marchal G, Suetens P (1997): Multimodality image registration by maximization of mutual information. IEEE Trans Med Imaging 16:187–198.

Maldjian JA, Laurienti PJ, Burdette JB, Kraft RA (2003): An automated method for neuroanatomic and cytoarchitectonic atlas-based interrogation of fMRI data sets. NeuroImage 19: 1233–1239.

Mazzola L, Isnard J, Mauguière F (2006): Somatosensory and pain responses to stimulation of the second somatosensory area (SII) in humans. A comparison with SI and insular responses. Cereb Cortex 16:960–968.

Melzack R, Casey KL (1968): Sensory, motivational, and central control determinants of pain. In: Kenshalo DR, editor. The Skin Senses. Springfield, IL: Charles C Thomas Publisher. pp 423–443.

Mesulam MM, Mufson EJ (1982): Insula of the old world monkey. III. Efferent cortical output and comments on function. J Comp Neurol 212:38–52.

Moont R, Crispel Y, Lev R, Pud D, Yarnitsky D (2011): Temporal changes in cortical activation during conditioned pain modulation (CPM), a LORETA study. Pain 152:1469–1477.

Nieuwenhuys R (2012): The insular cortex: A review. In: Hofman MA, Falk D, editors. Prog Brain Res 195:123–163.

Nunez, Srinivasan (2006): Electric Fields of the Brain—The Neurophysics of EEG. Oxford Univ Press. Print ISBN-13: 9780195050387.

Ohara S, Crone NE, Weiss N, Treede RD, Lenz FA (2004): Amplitudes of laser evoked potential recorded from primary somatosensory, parasylvian and medial frontal cortex are graded with stimulus intensity. Pain 110:318–328.

Ohara S, Anderson WS, Lawson HC, Lee HT, Lenz FA (2006): Endogenous and exogenous modulators of potentials evoked by a painful cutaneous laser (LEPs). Acta Neurochir Suppl 99: 77–79.

Ohara S, Crone NE, Weiss N, Kim JH, Lenz FA (2008): Analysis of synchrony demonstrates that the presence of "pain networks" prior to a noxious stimulus can enable the perception of pain in response to that stimulus. Exp Brain Res 185: 353–358.

Omigie D, Dellacherie D, Hasboun D, Clement S, Baulac M, Adam C, Samson S (2015): Intracranial markers of emotional valence processing and judgments in music. Cogn Neurosci 6: 16–23.

Ostrowsky K, Magnin M, Ryvlin P, Isnard J, Guénot M, Mauguière F (2002): Representation of pain and somatic sensation in the human insula: A study of responses to direct electrical cortical stimulation. Cereb Cortex 12:376–385.

Parvizi J, Van Hoesen GW, Buckwalter J, Damasio A (2006): Neural connections of the posteromedial cortex in the macaque. Proc Natl Acad Sci USA 103:1563–1568.

Perchet C, Frot M, Charmarty A, Flores C, Mazza S, Magnin M, Garcia-Larrea L (2012): Do we activate specifically somatosensory thin fibres with the concentric planar electrode? A scalp and intracranial EEG study. Pain 153:1244–1252.

Pessoa L (2008): On the relationship between emotion and cognition. Nat Rev Neurosci 9:148–158.

Peyron R, Laurent B, García-Larrea L (2000): Functional imaging of brain responses to pain. A review and meta-analysis. Neurophysiol Clin 30:263–288.

Peyron R, Faillenot I, Mertens P, Laurent B, Garcia-Larrea L (2007): Motor cortex stimulation in neuropathic pain. Correlations between analgesic effect and hemodynamic changes in the brain. A PET study. Neuroimage 34:310–321.

Rees G, Wojciulik E, Clarke K, Husain M, Frith C, Driver J (2000): Unconscious activation of visual cortex in the damaged right hemisphere of a parietal patient with extinction. Brain 123: 1624–1633.

Rorden C, Brett M (2000): Stereotaxic display of brain lesions. Behav Neurol 12:191–200.

Sato W, Kochiyama T, Uono S, Matsuda K, Usui K, Inoue Y, Toichi M (2013): Rapid and multiple-stage activation of the human amygdala for processing facial signals. Commun Integr Biol 6:e24562.

Schweinhardt P, Lee M, Tracey I (2006): Imaging pain in patients: Is it meaningful? Curr Opin Neurol 19:392–400.

Shipp S (2003): The functional logic of cortico-pulvinar connections. Philos Trans R Soc Lond B Biol Sci 358:1605–1624.

Siedenberg R, Treede RD (1996): Laser-evoked potentials: Exogenous and endogenous components. Electroencephalogr Clin Neurophysiol 100:240–249.

Talairach J, Bancaud J (1973): Stereotactic approach to epilepsy: Methodology of anatomo-functional stereotaxic investigations. Prog Neurol Surg 5:297–354.

Talairach J, Tournoux P (1988): Co-Planar Stereotaxic Atlas of the Human Brain: 3-Dimensional Proportional System: An Approach to Cerebral Imaging. Stuttgart (Germany), Thieme.

Tracey I, Mantyh PW (2007): The cerebral signature for pain perception and its modulation. Neuron 55:377–391.

Troiani V, Price ET, Schultz RT (2014): Un seen fearful faces promote amygdala guidance of attention. Soc Cogn Affect Neurosci 9:133–140.

Veinante P, Yalcin I, Barrot M (2013): The amygdala between sensation and affect: a role in pain. J Mol Psychiatry 1:9–14.

Vogt BA (2005): Pain and emotion interactions in subregions of the cingulate gyrus. Nat Rev Neurosci 6:533–544.

Vuilleumier P, Amony JL, Clarcke K, Husain M, Driver J, Dolan RJ (2002): Neural response to emotional faces with and without awareness: Event-related fMRI in a parietal patient with visual extinction and spatial neglect. Neuropsychologia 40: 2156–2166.

Willoch F, Gamringer U, Medele R, Steude U, Tölle TR, PET Activation Study (2003): Analgesia by electrostimulation of the trigeminal ganglion in patients with trigeminopathic pain: A PET activation study. Pain 103:119–130.

Zambreanu L, Wise RG, Brooks JC, Iannetti GD, Tracey I (2005): A role for the brainstem in central sensitisation in humans. Evidence from functional magnetic resonance imaging. Pain 114:397–407.